Optik 127 (2016) 39–42

Contents lists available at ScienceDirect

Optik

journal homepage: www.elsevier.de/ijleo

Evaluation of the mirror surface figure error based on the SlopeRMS

Wang Fu-guo*, An Qi-chang[1], Yang Fei[1]

Changchun Institute of Optics, Fine Mechanics and Physics, Chinese Academy of Sciences, Photoelectric Detection Department, Dong Nanhu Road 3888, Changchun 130033, Jilin, China

ARTICLE INFO

Article history:
Received 30 November 2014
Accepted 29 September 2015

Keywords:
Mirror surface figure error
SlopeRMS
Zernike polynomial
Power spectrum

ABSTRACT

The slope of the root mean square (SlopeRMS) can be applied to evaluate mid-spatial frequency mirror surface errors for larger aperture mirrors. In this paper, the SlopeRMS is analyzed from three different perspectives. First, the relationship between the SlopeRMS and the basis polynomials is discussed, and the mathematic relationship between the SlopeRMS and the standard orthogonal basis was obtained. Second, the SlopeRMS is analyzed by applying the Wiener process, with the results indicating that the ideal mirror surface error obeys the Gauss distribution law. Then, a power spectrum analysis method based on the SlopeRMS is proposed. The discrete random variables for describing the coma, astigmatism and quatrefoil were analyzed and the spectral energy distribution for the Zernike polynomials is discussed. Finally, by processing the error data of the Thirty Meter Telescope tertiary mirror surface figure, the frequency domain energy distribution of the actual mirror surface figure was obtained.

1. Introduction

A variety of methods exists to evaluate the surface figure error of reflective mirrors. As a traditional evaluation method, the root mean square (RMS) is typically used to describe the surface figure error of small aperture mirrors. Because the size of the grinding tools and the size of the optical components are similar, it can be applied to describe the simplest optical characteristics [1,2].

However, for large aperture reflective mirrors, this evaluation method faces several limitations. First, the small size of the grinding tools that are employed to polish the large aperture mirror will produce sub-aperture scale and mid-spatial frequencies, especially for aspheric surfaces and free surfaces. Particularly the grinding smoothness depends on a uniform distribution caused by the tools and the holding pressure time. Second, a multi-point support is always used for large aperture mirrors. As the number of support points increases, the mirrors will become more prone to mid-spatial frequencies. These mid-spatial frequencies produced by fringe irregularities are several times smaller than the optical element aperture, but larger than the surface's precision structure, i.e. the mirror surface roughness [3,4].

For different spatial frequency mirror surface figure errors, different evaluation methods produce different results. Fig. 1 shows a schematic illustration of two different optical surface figure errors. The optical surface of mirror A exhibits low frequency errors, while the optical surface of mirror B shows high frequency errors. When using the traditional RMS optical surface evaluation method, the RMS value is relatively large for mirror A, and relatively small for mirror B, and, consequentially, mirror A is unqualified, and mirror B is qualified. However, mirror A mainly exhibits low frequency errors, which can be easily corrected by applying adaptive optics, whereas the high frequency errors of mirror B are difficult to correct by adaptive optics. Therefore, the RMS evaluation method has its limitations for large aperture mirrors. In contrast, if using the slope of the root mean square (SlopeRMS) to evaluate the mirror surface error, the SlopeRMS value obtained for mirror A is small, and the SlopeRMS obtained for mirror B is large. Thus, mirror A is qualified, and mirror B is unqualified [1–4].

For large aperture mirrors, the surface figure test and evaluation directly affects the manufacturing accuracy and imaging quality [5,6]. The RMS test shows obvious shortcomings for evaluating large aperture mirrors. In recent years, some researchers therefore proposed using the SlopeRMS to evaluate the mirror surface error in the time domain. Although it can control rigid body displacements and reflect a wide range of roughnesses [7,8], for small scale shakes, there will be dramatic fluctuations. Therefore, an analysis based on the frequency-domain is necessary.

2. Mathematical analysis of the SlopeRMS

2.1. SlopeRMS and basis polynomials

Low order wave front errors are always fitted by basis polynomials. More precisely, the wave front error can be described by discrete index basis polynomials:

* Corresponding author. Tel.: +86 0431 86708871-613.
E-mail address: wfg109@163.com (W. Fu-guo).
[1] Tel.: +86 043186178215.

http://dx.doi.org/10.1016/j.ijleo.2015.09.244

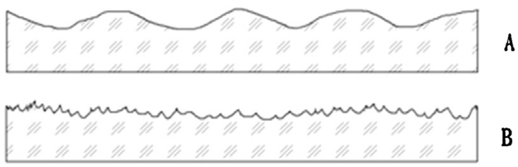

Fig. 1. Schematic illustration of two different mirror surface figures with (A) low-frequency errors and (B) high-frequency errors, respectively.

$$\Phi(m,n)=\sum a_{uv}W_{uv}(m,n) \tag{1}$$

where a_{uv} is the basis fitting coefficient and $W_{uv}(m,n)$ denotes the discrete index basis.

For a $N\times N$ sampling aperture, $W_{uv}(m,n)$ can be expressed by

$$W_{uv}(m,n)=\frac{1}{N\times N}\exp\left[\frac{2\pi j}{N}(um+vn)\right] \tag{2}$$

For convenience, only the imaginary component is considered in the one dimensional case, resulting in a standard sine polynomial. If the wave front error energy is constant, the RMS cannot be used to comprehensively reflect its dynamic performance. Therefore, the SlopeRMS is applied to address this problem:

$$\Phi=A\sin(2\pi fx) \tag{3}$$

with

$$\begin{aligned}(\nabla\Phi)^2&=(\nabla A\sin(2\pi fx))^2\\&=4A^2\pi^2f^2\cos^2(2\pi fx)\\ \left\langle\nabla\Phi^2\right\rangle&=\frac{2A^2\pi f\displaystyle\int_0^{1/f}\cos^2(2\pi fx)2\pi f\,dx}{1/f}\\&=2A^2\pi^2f^2\end{aligned} \tag{4}$$

For the standard sine polynomial in Eq. (3), the wave front error is constant, i.e. $\text{RMS}_\Phi=A$. Its SlopeRMS can be expressed by Eq. (6):

$$\Phi=\sqrt{2}A\sin(2\pi fx) \tag{5}$$

$$\text{slopeRMS}=\sqrt{2}\pi fA_{(2)} \tag{6}$$

It is generally assumed that the wave front error is a linear combination of two standard sine polynomials, as illustrated by Fig. 2, and its SlopeRMS can be expressed as follows:

$$\Phi=\alpha\sqrt{2}A\sin(2\pi fx)+\beta\sqrt{2}A\sin(2\pi fx)$$

$$\text{slopeRMS}^2=\left(\sqrt{2\alpha^2+8\beta^2\pi Af}\right)^2=\alpha^2 2f^2A^2+\beta^2 8f^2A^2$$

An extension of this construction to rank N yields:

$$\text{slopeRMS}^2=\sum_i^N c_i^2\text{slopeRMS}_i^2 \tag{7}$$

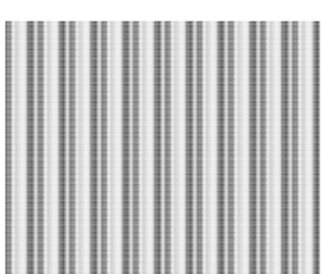

Fig. 2. Illustration of the multiplied wave front error.

This suggests that, if the wave front error is expressed by a standard orthogonal basis such as a standard sine polynomial, every item's SlopeRMS can be calculated individually, with the total SlopeRMS then obtained by summation. In the actual engineering application, some item's SlopeRMS can be first calculated as well, and then the total SlopeRMS can be obtained.

2.2. Ideal surface figure and Wiener process

For the surface figure of a reflective mirror, even for an absolutely ideal surface, the measurement instrument will produce an unavoidable error that will affect the mirror surface data; on the other hand, because of other uncontrollable factors (pressure disc jitter, thermal motion of magnetron fluid particles, random motion of beam particles), the actual surface figure will contain irregular fluctuations after the mirror has been polished.

The mathematical model of the Wiener Process was proposed by Einstein to analyze Brownian movement, essentially capturing the irregular movement by using a set of mathematical rules. This paper will analyze the mirror surface figure by referring to the Wiener process.

According to the basic assumptions of the Wiener process, in the measurement range, the mirror surface slope is zero at the starting point, whereas the surface slope has the following properties:

(1) Each coordinate component of the mirror surface slope $w(d_1)-w(u_1), w(d_2)-w(u_2), \ldots, w(d_n)-w(u_n)$ is independent. For one of the components, it is denoted as $w(l)$, while for arbitrary mutually disjoint regions, it is denoted as $[d_1,u_1],[d_2,u_2],\ldots,[d_n,u_n]$.
(2) The ideal error should be symmetrically distributed, so that $E\left\{w(l)\right\}=0$.
(3) The $w(l+\Delta)-w(l)$ distribution does not depend on l. Furthermore, $\sigma^2(\Delta)=E\left\{(w(l+\Delta)-w(l))^2\right\}$ exists and is the continuous function of Δ. As a result

$$\Phi(l,\lambda)=E\left\{e^{i\lambda w(l)}\right\}=\int_{\infty}^{+\infty}e^{i\lambda x}f(l,x)\,dx \tag{8}$$

and

$$\sigma^2(l)=E\left\{[w(l)-w(0)]^2\right\}=E\left\{w^2(l)\right\}=\int_{-\infty}^{+\infty}x^2f(l,x)\,dx \tag{9}$$

Then,

$$\begin{aligned}\sigma^2(l+s)&=E\left\{[w(l+s)-w(l)+w(l)-w(0)]^2\right\}\\&=E\left\{[w(l+s)-w(l)]^2\right\}+E\left\{w^2(l)\right\}=\sigma^2(s)+\sigma^2(l)\end{aligned} \tag{10}$$

$$\sigma^2(l)=Cl(C>0) \tag{11}$$

$$\Phi(l+s,\lambda)-\Phi(l,\lambda)=\Phi(l,\lambda)E\left\{e^{i\lambda w(s)-w(0))}-1\right\} \tag{12}$$

and

$$e^{iv}\approx 1+iv-\frac{v^2}{2} \tag{13}$$

Therefore:

$$\frac{\Phi(l+s,\lambda)-\Phi(l,\lambda)}{s}\approx\frac{1}{2}\lambda^2\Phi(l,\lambda)C \tag{14}$$

If $s\to o$, then

$$\frac{\partial\Phi(l,\lambda)}{\partial l}=-\frac{1}{2}\lambda^2\Phi(l,\lambda)C \tag{15}$$

Since $\Phi(0,\lambda)=1$